

Original Research

Modeling Underwater Noise Levels in the Slovenian Sea

Andreja Popit^{1*}, Luka Čurovič²

¹Andreja Popit, Institute for Water of the Republic of Slovenia, Einspielerjeva 6, 1000 Ljubljana, Slovenia

²Luka Čurovič, University of Ljubljana, Faculty of Mechanical Engineering, Aškerčeva 6, 1000 Ljubljana, Slovenia

Received: 12 May 2021

Accepted: 3 March 2022

Abstract

Underwater noise pollution due to marine traffic can have adverse effects on marine animals. This is the first study of modeling underwater noise levels from shipping in the Slovenian Sea. The aim of the study was to select and develop an appropriate methodology for modeling underwater noise levels. The logarithmic model was used to describe the range-dependent attenuation of low-frequency sound. The parameters of the model were determined from the transmission loss function calculated along ten selected cross sections across the North Adriatic using the parabolic equation. The difference between the measured and modeled levels was within ± 5 dB. However, the model was able to identify trends in underwater noise levels that could not be identified by the measurements, suggesting that noise maps could provide a basis for management purposes. In building the model, we found that the modeled values are mainly affected by the speed of the ships. Therefore, adjusting the speed of ships could be an effective measure to be taken into account for controlling underwater noise from shipping in the world's seas and oceans.

Keywords: underwater noise, shallow sea, parabolic equation model, mitigation measure

Introduction

State of the Art Knowledge on Underwater Acoustic Propagation Modeling

Good environmental status of marine waters for descriptor 11 is achieved if introduction of energy, including underwater noise, is at levels that do not adversely affect the marine environment [1]. In this regard, the Commission Decision [1] requires an annual average underwater noise levels in marine environment

to be assessed from direct measurements or inferred from a model.

Noise levels arising from anthropogenic activities should be modeled and their potential impact on species of interest within the affected area then evaluated. The basic objective of noise modeling for environmental impact assessment is to predict how much noise a particular activity will generate in the surroundings. More formally, the aim is to model the received noise level (RL) at a given point (or points), based on the source level (SL), and on the amount of sound energy that is lost as the sound wave propagates from the source to the receiver (propagation loss; PL) [2]. The relationship between these quantities is written in the classic sonar equation [3]:

*e-mail: andreja.popit@izvrs.si

$$RL = SL - PL \tag{1}$$

Propagation loss (*PL*) is often estimated using the simple spreading law expressed in the equation:

$$PL = N \log_{10}(R) \tag{2}$$

where *R* is the distance from the noise source in meters and *N* is a scaling factor. Since this simplistic approach does not account for complexities in the environment, it can only produce reasonable predictions for uncomplicated propagation scenarios, for example range independent environments where extensive measurements from the study site are available to derive the value of *N* [4].

The first step in carrying out a noise assessment is to identify an appropriate sound propagation loss model. A large number of propagation models have been developed, based on several underlying mathematical methods, such as ray theory, normal mode, wave number integration, parabolic equation, an energy flux model or finite difference or finite element model [4-6]. No single model is applicable to all acoustic frequencies and environments (Table 1).

Physical or numerical models have been developed for several common noise sources, including pile driving [7,8,9], seismic air guns and shipping [10-13].

The most common propagation models used for underwater noise predictions are presented in Table 1. Important factors to be considered, besides the computational requirements, are the frequencies of sound to be modeled, the water depth, and whether spatial variation in the environment is significant (known as range dependent or range independent variables). Each of these factors should influence model selection (Table 1). For large-scale applications, such as sound maps, it is important that field measurements are undertaken to validate the assumption that model predictions are accurate [2, 4, 6].

Ray model is limited in accuracy at low frequencies (typically below 200 Hz) where reflection and scattering are significant and where sound absorption

in the seabed occurs. The Ray model approach performs poorly when there are discontinuous sound speed profiles. Ray model is suitable for arbitrary range-dependent environments, deep waters and higher frequencies [4].

Normal mode approach is best suited to mildly range-dependent environments and at lower frequencies. It is used extensively in both shallow and deep water [4].

There are two types of parabolic equation (PE) models available – the split-step Fast Fourier Transform solution and the Padé expansion solution. The PE model is an efficient solution that is suitable for range-dependent environments, discontinuous sound speed profiles and is commonly used in shallow and deep water [4]. The PE computational requirements increase with frequency squared and therefore the PE model is generally used at frequencies less than 1 kHz.

Propagation of sound in shallow waters is significantly influenced by the bathymetry, the seabed sediment properties and sea surface, due to the repeated reflections and scattering. Important parameters for modeling sound propagation are the sediment density, the sound speed and the acoustic attenuation [2, 4].

Global bathymetric data can be obtained on the website of General Bathymetric Chart of the Oceans (GEBCO) [14] or on the website of TOPEX [15]. Seabed data can be provided by EMODNET database [16]. For modeling purpose, the seabed data have to be converted into acoustic properties [2]. The sound speed profile can be measured *in situ*, and can also be obtained from the database of the National Center for Environmental Information [17], which provides information about the geographic and seasonal variability.

The Commission Decision [1] requires an annual average underwater noise levels in marine environment to be assessed from direct measurements or inferred from a model. The aim of our study in this regard was to select and develop a proper methodology for modeling underwater noise levels in the shallow Slovenian sea in the period from 2015 until 2018, in order to be able to study the noise hot spots due to ship traffic.

Table 1. Applicability of the most common propagation models according to water depth, acoustic frequency, and range dependence (*RI* = range independent; *RD* = range dependent). Black cells indicate modeling approach is applicable and computationally efficient; grey cells indicate limitations in accuracy or computational efficiency; white cells indicate that the modeling approach is neither applicable nor practicable [5].

Model approach	Example algorithm	Applications							
		Shallow water				Deep water			
		Low frequency		High frequency		Low frequency		High frequency	
		RI	RD	RI	RD	RI	RD	RI	RD
Ray	BELLHOP (Porter and Liu, 1994)			Grey	Black	Grey	Grey	Black	Black
Normal mode	KRAKEN (Porter, 1992)	Black	Grey	Black	Grey	Black	Grey	Grey	White
Parabolic equation	RAM (Collins, 1993)	Grey	Black	White	White	Grey	Black	Grey	Grey

This study is important for determination of the optimal mitigating measures for achieving the good environmental status of the marine environment, which is an objective of the Marine Strategy Framework Directive [18].

Materials and Methods

Methodology for Determining a Source Level and Selection of a Proper Sound Propagation Model

Underwater noise due to maritime shipping comes mainly from the cavitation generated by the ship's propeller and from the ship vibrations [19]. The source level (*SL*) can be estimated using a physical or numerical model of the noise source, or by using field measurements of received level to calculate the source level using an appropriate propagation model [2, 20]. For the underwater noise mapping in this study, values of the source level of ships were taken from the literature. The source level depends on the type of ship, its length and speed. For modeling purposes, a typical spectral source level for an individual ship type was used. A source level was determined using a RANDI (Research Ambient Noise Directionality) model based on the Ross equation [11, 12, 13, 20], which is most often used in the literature:

$$SL(f, v, l) = SL_0(f) + 60 \log(v/12) + 20 \log(l/300) + df \cdot dl + 3$$

$$L_{eq}(t) = 10 \log_{10} \left(\frac{P_{rms}}{p_0} \right)^2 = 20 \log_{10} \left(\frac{P_{rms}}{p_0} \right) \tag{3}$$

Table 2. Classification of ships according to their length and speed.

Ship class	L1	L2	L3	L4	L5
Ship length (m) [11]	0–10	10–25	25–50	50–100	>100
Speed of ship (kt) [21]	5	5	5	5	5
Ship length (m) used in the model [11]	7.8	18.6	38.9	77.8	156

where *l* is the length of the ship in feet, *f* is the frequency, *v* is the speed of the ship in knots (kt), *SL*₀ is the reference source level, *df* and *dl* are given by the equations [11]:

$$df = \begin{cases} 8.1 & 0 \leq f \leq 28.4 \text{ Hz} \\ 22.3 - 9.77 \log f & 28.4 \text{ Hz} \leq f \leq 191.6 \text{ Hz} \end{cases} \tag{4}$$

$$dl = l^{1.15} / 3643.0 \tag{5}$$

The source level (*SL*) in 1/3 octave band frequency spectrum for each ship class is shown in Fig. 1.

Ships can be distributed into several classes, depending on their length, speed and depth of the acoustic center of the source, with the help of Table 2. The speed and the length of the ship used to calculate the source level are given in Table 2 [11, 21].

Etter [5] developed a matrix based on the requirements that enables selection of a proper model

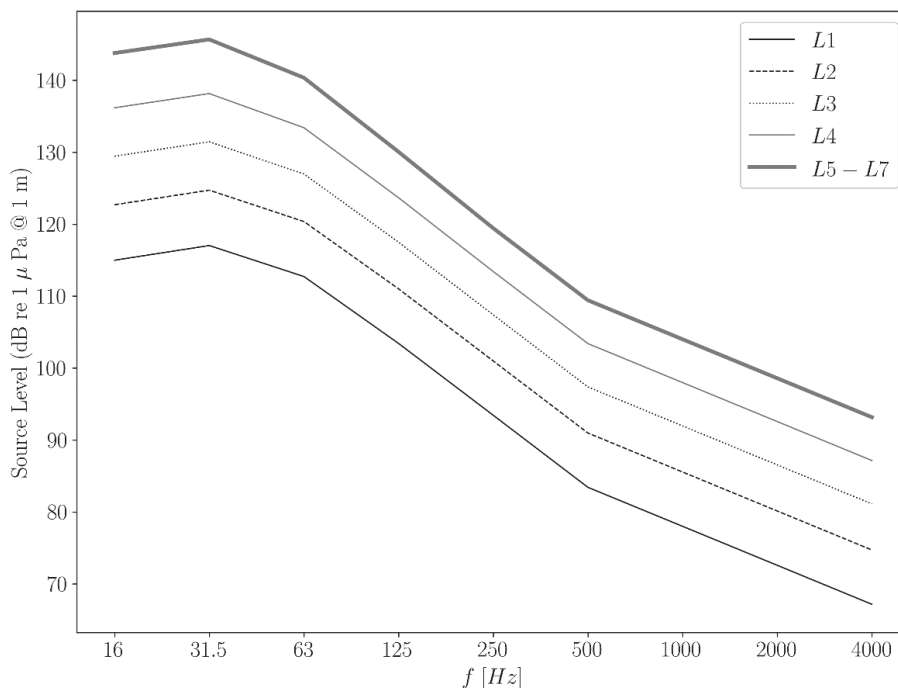


Fig. 1. Source level (*SL*) spectrum of individual ship class based on the Equation (3) [12].

(Table 1). A depth of 200 m is typically used, up to which the marine environment is considered to be shallow. In a shallow water sound interacts significantly with the seabed. Given this matrix, the use of the parabolic equation model (PE model) is recommended for shallow waters at low frequencies.

Methodology for Calculation the Sound Attenuation and Sound Pressure Levels

In the PE method, the Helmholtz equation is reduced to a parabolic equation with two variables. The method is useful for modeling the propagation of sound in media that do not change significantly with distance from the source, such as in the marine environment. The PE equation can be solved with the RAMGeo algorithm (RAM means Range-dependent Acoustic Model) that is implemented in the AcTUP software environment, which is an open source program [22]. The RAMGeo algorithm requires knowledge of certain parameters and quantities that affect sound propagation, thus the standard literature parameters were considered [20]:

- knowledge of bathymetry,
- sea roughness: 0 Beaufort on Beaufort scale,
- speed of sound at a depth of 2 m = 1516 m/s,
- speed of sound at a depth of 23 m = 1540 m/s,
- surface water density = 1024 kg/m³,
- water density at depth of 23 m = 1024 kg/m³,
- velocity of longitudinal waves in the sediment 1800 m/s,
- sediment density 2048 kg/m³,
- sound absorption in the sediment 0.5 k/m³.

Data on bathymetry were obtained through a database accessible on the TOPEX website [15]. Data on sea depths are given in steps of 30 degrees, which means a resolution of approximately 1 km x 1 km was used because high resolution data were not available. The bathymetry used between latitudes 45°N and 46°N and longitudes 13°E and 14°E is shown in Fig. 2.

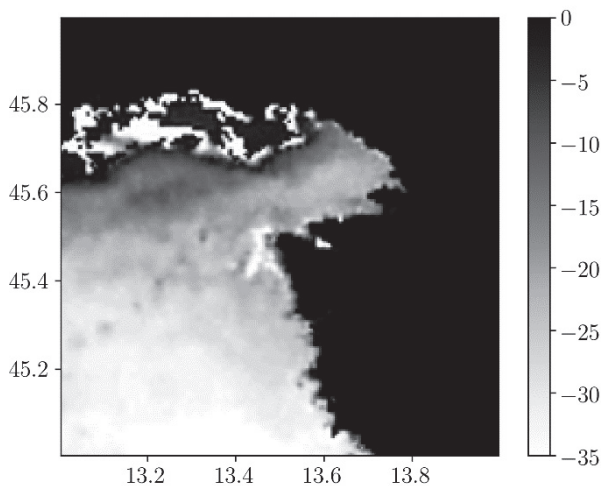


Fig. 2. Bathymetry based on a global database of bathymetry and altitudes at a spatial angle resolution of 30 degrees [15].

The computational complexity of the RAMGeo algorithm is too great to be able to verify the propagation of a sound wave in all directions from the noise source for each noise source. We therefore, chose the principle used in modeling ship noise in the area of Northern Colombia in Canada [13] and we analyzed sound propagation in a few selected typical directions. In our model, 10 cross-sections were selected [19], as shown in Fig. 3, on the basis of which, the sound attenuation, as a function of distance and depth, was determined.

Along each cross-section, the parabolic equation (PE) was solved using the RAMGeo algorithm and the dependence of the function TL (sound attenuation) on the distance to the source (r) and the water depth (z) was determined ($TL = TL(r, z)$). In our case, the minimum value of TL was taken at each distance from the source r . This gives a conservative estimate for the noise propagation as a function of distance from the source.

Using the described procedure, TL was determined as a function of r for each individual frequency (f) and for each cross-section. In this way, a multitude of TL functions at individual frequency was obtained. In doing so, it was concluded that the individual curves do not differ significantly from each other. At each frequency, the median $TL(r)$ was then determined and the curves $TL(r)$ for each frequency (f) obtained. To each of the curves the following shape of a curve could be assigned [13]:

$$TL(r, f) = a_1 \log r + a_2 r \quad (6)$$

where a_1 and a_2 are the coefficients obtained by adjusting the curve using the least squares method. The propagation of low-frequency noise (63 Hz, 125 Hz) in a shallow channel is approximately cylindrical (the a_1 coefficient is approximately 10).

For 63 Hz the following equation was developed (R squared value is also shown):

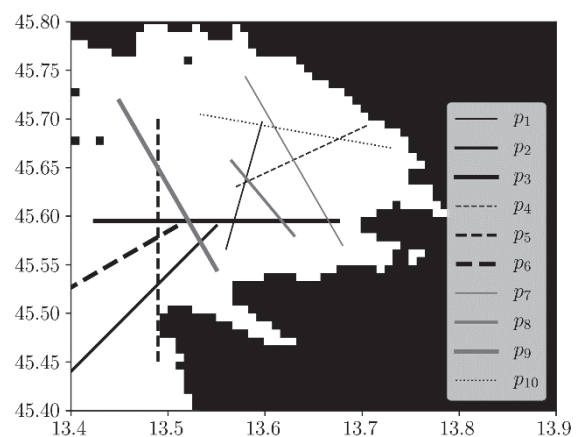


Fig. 3. Ten cross-sections used in our model.

$$TL(r, f) = 11.2000 \log r - 0.00020 r \quad (R^2 = 0.9748) \quad (7)$$

For 125 Hz the following equation was developed:

$$L(r, f) = 10.9736 \log r - 0.00001 r \quad (R^2 = 0.9912) \quad (8)$$

$TL(r, f)$ values at depths below the height determined by the cut-off frequency were not used for the least squares method. The cut-off can be identified as a step in the $TL(r)$ plot. The average height of the step was evaluated as 1.5 dB.

Sound attenuation determination due to sound absorption is in practice most often determined using the Francois Garrison model [23], which takes into account viscosity, chemical relaxation, wave frequency, salinity, temperature, depth and pH value of water. The model is mathematically written with the equation:

$$TL_a = \frac{\alpha r}{1000} \quad (9)$$

where r is the distance of the investigated location from the noise source in km. α is the absorption coefficient in dB/km given by the equation in [23]:

$$\alpha = 0.106 \frac{f_1 f^2}{f_1^2 + f^2} e^{\frac{pH-8}{0.56}} + 0.52 \left(1 + \frac{T}{43}\right) \frac{S}{35} \frac{f_2 f^2}{f_2^2 + f^2} e^{-\frac{z}{6}} + 4.9 \cdot 10^{-4} f^2 e^{-\frac{T}{27} + \frac{S}{17}} \quad (10)$$

where f is the frequency in kHz, α is the absorption coefficient in dB/km, T is the temperature, S is the salinity in per mille (‰), z is the depth and the coefficients f_1 and f_2 are [23]:

$$f_1 = 0.78(S/35)^{0.5} e^{T/26} \quad (11)$$

$$f_2 = 42 e^{T/17} \quad (12)$$

To determine the sound pressure level at the immission point (the point at which the receiver is located), it is necessary to consider whether the places where the source and the receiver are located are connected by the sea or there is a sound barrier between them (i.e. land). If the shortest path between the two points passes over the land then it was assumed that the source does not cause noise at that point. In doing so, the diffraction and reflection of the sound waves were neglected.

Sound attenuation was calculated for all connections between the noise source (vessel) and immission points (receiver) that do not pass over the land. The sound pressure level at each point was calculated as in [13]:

$$RL = SL(r_0, f) - TL(r, f) - TL_a(r, f) \quad (13)$$

where the level of the SL source was determined by Equation (3), TL is the attenuation of sound given by Equations (7) and (8). TL_a is the frequency-dependent loss of sound intensity due to the absorption calculated by the empirical Equation (9). In Equation (13) r_0 is the reference distance equal to 1 m, f is the wave frequency, r the distance, T the temperature, S the salinity and z the depth. In addition, the properties of sound waves in shallow sea were taken into account. In shallow waters and canals, low-frequency signals cannot propagate unhindered due to the changed impedance. Because of this, a critical frequency f_0 (cut off frequency) is introduced in shallow waters where sound waves propagate poorly. The critical frequency can be determined from the equation given in [24]:

$$f_0 = \frac{c_0}{4H \sin \theta_c} \quad (14)$$

where c_0 is the speed of sound in water and θ_c is the critical angle given by the equation in [24]:

$$\theta_c = \cos^{-1} \frac{c_0}{c_1} \quad (15)$$

where c_1 is the speed of sound in marine sediment. Frequencies that are lower than the critical frequency propagate poorly through the channel of depth H .

Algorithm for the Noise Map Calculation

The noise map showing the spatial distribution of the noise levels in 1/3 octave bands with center frequencies at 63 Hz and 125 Hz was constructed according to the following procedure:

- First, the cell coordinate was entered in the form of geographic coordinates (Lon and Lat in degrees) where the ships were located.
- Secondly, the number of ships located in the cell was entered.
- Thirdly, the source level of the ship or group of ships was selected. The source level corresponding to group 2 (L_2 in Fig. 1) was used in this study.
- Fourthly, the matrix of distances between the cell where the ship was located and the remaining cells of the considered area was calculated.
- Fifthly, the profiles between the cell where the ship was located and the remaining cells of the considered area were calculated. In this way it was checked whether there is land between the cell with the ship and the area of immission.
- Sixthly, the noise level at the receiver location was calculated as follows:
 - a) If the height of the water column at the point of reception was higher than that determined by the critical frequency, Equation (13) was used.
 - b) If the height of the water column at the point of reception was lower than the height determined by the critical frequency, Equation (13) was used and an additional 1.5 dB were subtracted. In this way,

the poor propagation of sound below the cut off frequency was taken into account.

- c) If the cell where the source was located coincided with the cell where the receiver was located, a distance of 0.3 km was used that corresponds to the average distance of points within the cell to the cell center of the dimension 1 km x 1 km [13].
- Seventhly, the total noise level (noise emitted by all the ships, RL_{total}) was calculated for each cell using the equation:

$$RL_{total} = 10 \times \log_{10} \left(\sum_{i=0}^{i=N} 10^{0.1RL_i} \right) \quad (16)$$

where RL_i is the noise level in a single cell caused by the i -th ship.

Distribution of the Ship Traffic

Data on ship locations were obtained from the AIS (Automatic Information System) and were used to determine the ship densities at the following areas [25]:

- within a radius of 2 nautical miles (NM, 1 NM is 1852 m) from the measuring station at Debeli rtič (Lat: 45.5912°, Lon: 13.6997°);
- within a radius of 5 NM from the measuring station at Debeli rtič;
- in the Gulf of Trieste and
- in the Gulf of Venice.

In the case of ships located between 0 and 5 NM from the measuring station, it was assumed that ships were more likely to be located in the area of the ship corridors. Shipping routes were determined on the basis of analysis of the navigation of the ships sailing into or from the Gulf of Koper and on the route Trieste-Koper.

In this study, noise maps were constructed for the average ship densities during each year. Noise was calculated in a spatial mesh with cells of dimension 1 km x 1 km. In the model calculation, it was taken into account that the ships were located inside the cells, as shown in Fig. 4.

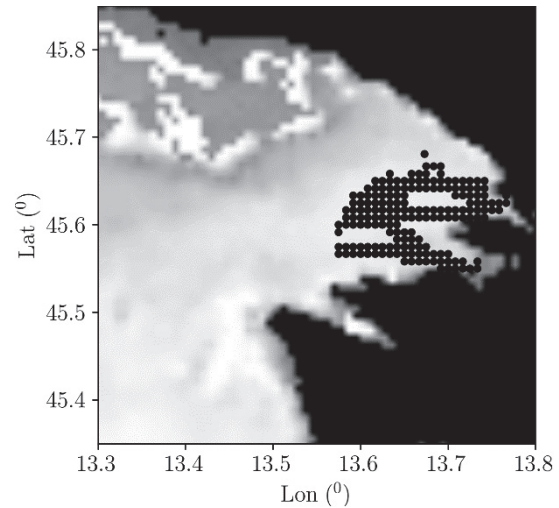


Fig. 4. Distribution of the ships in the radii of 2 NM and 5 NM from the measuring station of the underwater noise at Debeli rtič, Slovenia.

In accordance with the distribution of the noise sources along the shipping lanes, the source levels (SL) were evenly distributed over the area on which the ships were located. When calculating the source level of an individual cell (SL'), the surface distribution of the sources of noise had to be taken into account. In the case of the ships located between 0 NM and 5 NM from the measuring station, this was done using the following equation:

$$SL' = SL - 10 \log(S/S_0) + 10 \log(N/N_0) \quad (17)$$

where SL is the source level, S is the surface of the area where the ships were located, S_0 is the reference surface of 1 m², N is the number of ships within the area and N_0 is the reference number of ships ($N_0 = 1$).

The ships in the Gulf of Trieste were treated as a surface noise source for which Equation (17) was used. The ships in the Gulf of Venice were located at

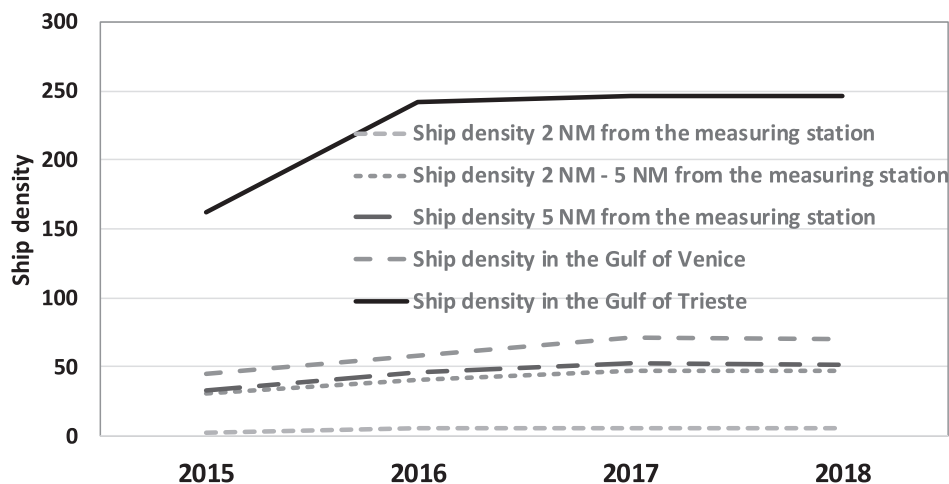


Fig. 5. Average ship densities in the period 2015-2018.

greater distances from the measuring station and thus considered as point sources within the gulf at the location with coordinates: Lat: 45.3167°, Lon: 13.0000°. The source level of the cell (SL') was calculated using the equation:

$$SL' = SL + 10 \log(N/N_0) \quad (18)$$

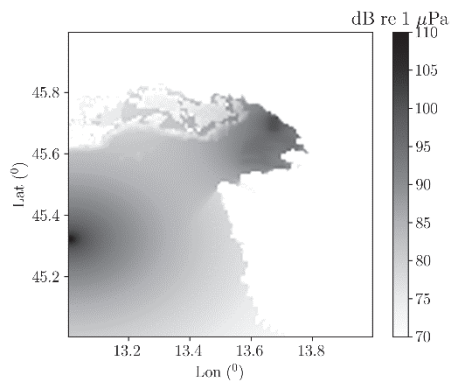


Fig. 6. Map of noise levels in 1/3 octave band with a center frequency of 63 Hz for the year 2015.

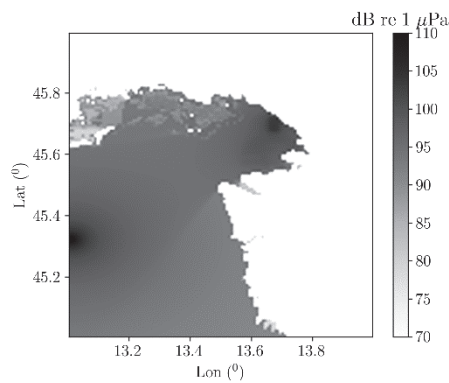


Fig. 7. Map of noise levels in 1/3 octave band with a center frequency at 125 Hz for the year 2015.

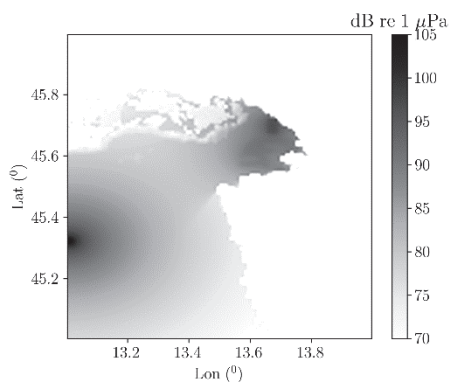


Fig. 8. Map of noise levels in 1/3 octave band with a center frequency of 63 Hz for the year 2016.

Results

Ship Densities

The average ship densities in the period 2015-2018 were calculated (Fig. 5). The density of ships increased significantly in the year 2016 and then stabilized. This trend is particularly visible in the case of the Gulf of Venice. The average ship density in the year 2015 was lower than those in the years 2016-2018.

Results of the Modeling

The results of the modeling were presented as underwater noise maps showing the spatial distribution of the underwater noise levels in 1/3 octave bands with center frequencies of 63 Hz and 125 Hz in 2015, 2016, 2017 and 2018 (Figs 6-13).

There was less shipping in the year 2015, than in the years 2016 to 2018, thus noise levels were also lower. Lower noise levels due to the shipping in the area of the Piran Bay were observed during the entire period between 2015 and 2018.

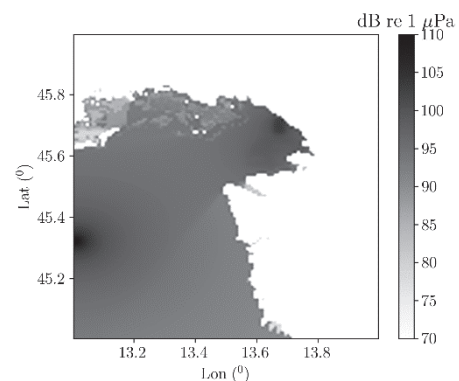


Fig. 9. Map of noise levels in 1/3 octave band with a center frequency of 125 Hz for the year 2016.

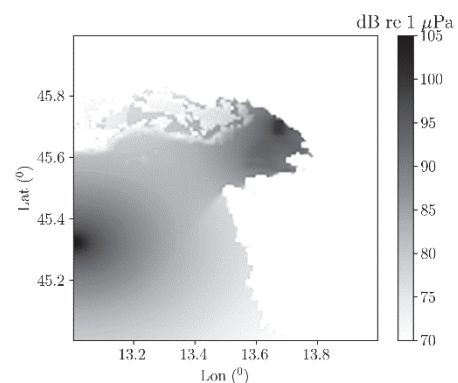


Fig. 10. Map of noise levels in 1/3 octave band with a center frequency of 63 Hz for the year 2017.

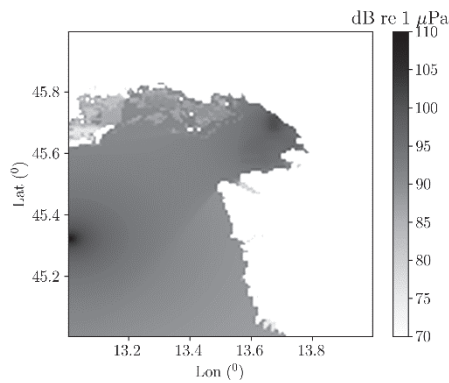


Fig. 11. Map of noise in 1/3 octave band with a center frequency of 125 Hz for the year 2017.

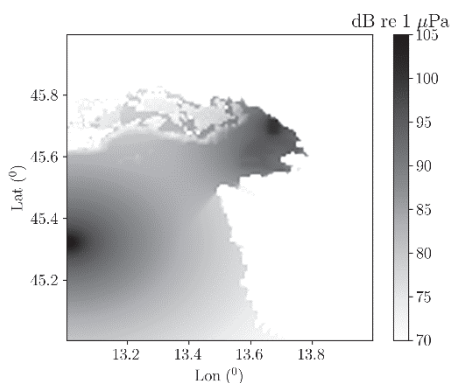


Fig. 12. Map of noise levels in 1/3 octave band with a center frequency of 63 Hz for the year 2018.

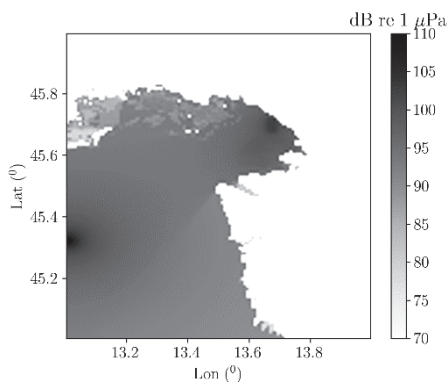


Fig. 13. Map of noise levels in 1/3 octave band with a center frequency of 125 Hz for the year 2018.

Discussion

Interpretation of the Results

Results of the modeling show that the underwater noise in the frequency range of 125 Hz is propagated better than the low-frequency noise at 63 Hz. This is due to the shallowness of the sea.

Trends in noise levels, noise hot spots and the quietest areas were studied in the Slovenian Sea based on the modeled maps of underwater noise (Figs 6-13). The modeled noise maps show only minor differences in the noise level distribution that is due to differences in the ship densities. The lowest underwater noise levels were observed in the year 2015, when there was less shipping traffic than in the other years.

Noise hot spots on the modeled spatial distributions of the noise levels in 1/3 octave bands, with center frequencies at 63 Hz and 125 Hz from 2015 to 2018 (Figs 6-13), were evident in the areas of Port of Koper and of the Gulf of Trieste. That was the result of the shipping to or from the Port of Koper and to or from the Port of Trieste.

The lowest levels of underwater noise in the Slovenian Sea on the modeled noise maps from 2015 to 2018 were observed in the area of the Piran Bay (Figs 6-13), which is located south of the main shipping routes. Furthermore, a map of sightings of the bottlenose dolphins (*Tursiops truncatus*) from January 2018 until September 2018 was used from the literature [26]. It was observed that the lowest modeled levels of underwater noise in 2018 (Figs 12 and 13) coincide with the sightings of the bottlenose dolphins from January until September 2018, which were more common in the southwestern part of the Slovenian Sea, away from the main shipping routes.

Critical Evaluation and Validation of the Model and Relation to other Studies

This is the first study of modeling underwater noise levels due to the ship traffic in the Slovenian Sea. For modeling underwater noise levels at low frequencies in the shallow seawater the parabolic equation model (PE model) was chosen based on the matrix developed by Etter (2009, 2012) and based on the studied acoustical propagation models from the literature [4, 6]. Sound propagation was analyzed in ten selected typical cross-sections according to the principle used in modeling ship noise in the similar study in the area of Northern Colombia in Canada [13], on the basis of which, the sound attenuation, as a function of distance and depth, was determined.

A scientifically important finding based on the developed propagation model is that modeled values were most influenced by the parameters that describe the noise emission or source level. The first of these was the speed of the ship that was included in Equation (3). Thus, adjusting the speed of ships could be used as an effective measure to control underwater noise from shipping in the world's seas and oceans.

The modeled values of the underwater noise in our study are approximation, due to the uncertainties involved in the computation as reported in the similar studies from the literature [2, 4, 6, 12]. For this reason, the results of the modeled underwater noise levels in 1/3 octave bands with center frequencies at 63 Hz

Table 3. The average measured underwater noise levels in 1/3 octave bands with center frequencies at 63 Hz and 125 Hz in the years 2015-2018 compared to modeled values.

Year	Measured underwater noise levels		Modeled underwater noise levels	
	$L_{eq,63\text{Hz}}$ (dB re μPa)	$L_{eq,125\text{Hz}}$ (dB re μPa)	$L_{eq,63\text{Hz}}$ (dB re μPa)	$L_{eq,125\text{Hz}}$ (dB re μPa)
2015	83.2	86.9	87.6	86.8
2016	99.8	96.2	88.8	88.2
2017	86.9	85.3	89.5	88.7
2018	89.5	95.1	89.5	88.7

and 125 Hz were validated with the measured underwater noise levels from the measuring station at Debeli rtič, Slovenia, between 2015 and 2018. The autonomous continuous noise measurements were performed using BK type 2250 sound level meter connected to BK type 8105 hydrophone using 48 kHz sampling frequency. The hydrophone was positioned approximately 4 m below the sea surface. The sound pressure levels in 63 Hz and 125 Hz bands were calculated for each hour and stored to USB disk. The results of these measurements are shown in Table 3. Underwater noise levels at the same location were calculated using the proposed model and data on ship densities (Table 3).

Deviation between the measured and the modeled underwater noise levels was large, especially in 2016, for both indicators and, in 2018, for the $L_{eq,125\text{Hz}}$. Similar discrepancies have been observed in the literature [27]. The observed deviation could be because the source levels of the ships were estimated based on the literature data [12] and because spatial distribution of the ships were estimated based on the shipping corridors. The model took into account constant values of some parameters (i.e. sound absorption in the sea floor and water, speed profile and temperature profile) that are, in reality, time- and space dependent. Furthermore, a large share of vessels in the northern Adriatic is assumed not to be detected with the AIS system, although they could contribute significantly to the measured noise levels. For this reason, these vessels could not be included in our model.

Despite the fact that not all input data were known and that the measuring station is located in a shallow sea, we can conclude that the difference between the measured values and the modelled calculations was within ± 5 dB. The exception was in the year 2016, in which the measured levels of the underwater noise were higher than those obtained by the model.

The PE model was used in a similar study for mapping cumulative noise from shipping in the western Canadian coast [12], where the standard deviation between the modeled and measured sound transmission loss was only 10 dB at 80 km (less at shorter ranges).

Close agreement of the modeled underwater low frequency ambient noise levels with the measured values was reported also in the study of the Great Barrier Reef Marine Park, Australia [28], in which noise levels were predicted using the normal mode model.

Furthermore, a case study in the Celtic Sea showed that application of the adaptive grid even improved the efficiency and accuracy (errors less than 0.5 dB) of modeling underwater noise from shipping using ray tracing or PE model [29].

Good agreement between the measurements and the modeled underwater noise levels were reported in the most recent study in the Northeast Atlantic [30] using energy-flux range-dependent model. This study demonstrated that shipping noise maps based on AIS ship-tracking data could make valid predictions of noise levels that could be suitable for policymaking and management.

The results of the underwater noise model in the Slovenian Sea show that the long-term $L_{eq,125\text{Hz}}$ levels were lower than $L_{eq,63\text{Hz}}$ levels and show an increase in noise levels between 2015 and 2018. However, no such trends were observed in the noise measurement data. These measurement results suggest that the assessment of shipping noise in shallow waters based on autonomous noise measurements is influenced by the presence of unwanted sound events due to local vessel traffic and weather conditions. Unwanted sound events and adverse weather conditions could also be the reason for the increased noise levels measured in 2016. The levels measured in 2016 are much higher than in other years, and the 10 dB increase cannot be explained by different vessel densities.

Measurement uncertainty should be improved by additional data processing, sound recording, and weather monitoring.

A more detailed measurement procedure would allow the identification and classification of the main noise sources, the validation of the noise map and the improvement of its accuracy.

We therefore conclude that modelled noise maps could provide a basis for management purposes to decide where mitigation measures should be taken.

Conclusions

This is the first study of modeling underwater noise levels due to the ship traffic in the Slovenian Sea. The model developed for underwater noise propagation at low frequencies in shallow seawater was based on a logarithmic model where the transmission loss was calculated as the mean transmission loss along 10 cross sections across the northern Adriatic Sea using a parabolic equation. The model developed for underwater noise propagation at low frequencies in the shallow seawater was based on the parabolic equation. Noise hot spots from 2015 to 2018 were observed in the areas of Port of Koper and of the Gulf of Trieste, which were the result of the shipping. In contrast, the lowest levels of underwater noise in the Slovenian Sea on the modeled noise maps from 2015 to 2018 were observed in the area of the Piran Bay, which is located south of the main shipping routes.

An important finding based on our developed propagation model is that modeled values were influenced mostly by the speed of the ships. Therefore, adjusting the speed of ships could be an effective measure to be taken into account for controlling underwater noise from shipping in the world's seas and oceans.

Based on our study, we conclude that modeled underwater noise levels and produced noise maps for the Slovenian Sea provide useful tool to allow the competent authorities to decide where mitigation measures may be applied to make noisy areas quieter.

In our future modeling, we will develop models based on a wider set of data that are provided by the AIS system (i.e. distribution of the ships, ship lengths and ship speeds), together with a higher spatial resolution.

Acknowledgments

This study was financed by the Slovenian Ministry for the Environment and Spatial Planning. Automatic Information System (AIS) data for the year 2015 were obtained from the European BALMAS project – with the permission of the Italian Coast Guard Headquarters, whereas AIS data for the period 2016-2018 were obtained by the Slovenian Maritime Administration.

Conflict of Interest

The authors declare no conflict of interest.

References

- Commission Decision of 17 May 2017 laying down criteria and methodological standards on good environmental status of marine waters and specifications and standardized methods for monitoring and assessment, and repealing Decision 2010/477/EU, Official Journal of the European Union, **848**, 2017.
- FARCAS A., THOMPSON P.M., MERCHANT N.D. Underwater noise modeling for environmental impact assessment. *Environmental Impact Assessment Review*, **57**, 114, 2016.
- URICK R.J. Principles of Underwater Sound. Third ed. McGraw-Hill, New York, 1983.
- WANG L., HEANEY K., PANGERC T., THEOBALD P., ROBINSON S., AINSLIE M. Review of underwater acoustic propagation models. NPL Report AIR (RES) 086, National Physical Laboratory, U.K., 2014.
- ETTER P.C. Review of ocean acoustic models. Proceedings of 20th International Congress in Acoustics – ICA, 2009.
- BORSANI J.F., FAULKNER R., MERCHANT N.D. Impacts of noise and use of propagation models to predict the recipient side of noise. Cefas contract report: C6082, Centre for Environment, Fisheries and Aquaculture Science, U.K., pp. 27, 2015.
- ZAMPOLLI M., NIJHOF M.J.J., JONG C.A.F., AINSLIE M.A., JANSEN E.H.W., QUESSON B.A.J. Validation of finite element computations for the quantitative prediction of underwater noise from impact pile driving. *J. Acoust. Soc. Am.*, **133** (1), 72, 2013.
- LIPPERT T., VON ESTORFF O. The significance of parameter uncertainties for the prediction of offshore pile driving noise. *J. Acoust. Soc. Am.*, **136** (5), 2463, 2014.
- FRICKE M.B., ROLFES R. Towards a complete physically based forecast model for underwater noise related to impact pile driving. *J. Acoust. Soc. Am.*, **137** (3), 1564, 2015.
- KELLETT P., TURAN O., INCECIK A. A study of numerical ship underwater noise prediction. *Ocean Engineering*, **66**, 113, 2013.
- ANSI Methods for measurement of impulsive noise (ANSI S12.7-1986). New York, Acoustical Society of America. Standard, 1986.
- ERBE C., MACGILLIVRAY A., WILLIAMS R. Mapping cumulative noise from shipping to inform marine spatial planning. *The Journal of the Acoustical Society of America*, **132** (5), 423, 2012.
- ERBE C., DUNCAN A., KOESSLER M. Modeling noise exposure statistics from current and projected shipping activity in northern British Columbia. Report submitted to WWF Canada by Curtin University, Australia, 2012.
- GEBCO. Available online: <http://www.gebco.net>. (accessed 15.3.2021).
- TOPEX. Available online: http://topex.ucsd.edu/WWW_html/srtm30_plus.html. (accessed 15.3.2021)
- EMODNET. Available online: <https://emodnet.eu/en>. (accessed 17.3.2021).
- CENTRES FOR ENVIRONMENTAL INFORMATION. Available online: <https://www.ncei.noaa.gov/products/ocean-climate-laboratory> (accessed 17.3.2021).
- Directive of the European Parliament and of the Council: Establishing a framework for community action in the field of marine environmental policy (Marine Strategy Framework Directive), Official Journal of the European Union, **56**, 2008.
- ANSI/ASA S12.64-2009/Part 1, Quantities and Procedures for Description and Measurement of Underwater Sound from Ships, Part 1, General Requirements. Standard, 2009.
- ROSS D. Mechanics of underwater noise. Elsevier, 2013.
- MARINETRAFFIC. Available online: <http://www.marinetraffic.com>. (accessed 18.3.2021).

22. CENTRE FOR MARINE SCIENCE AND TECHNOLOGY. Available online: <http://cmst.curtin.edu.au/products/underwater>. (accessed: 18.3.2021).
23. FRANCOIS R.E., GARRISON G.R. Sound absorption based on ocean measurements. Part ii: Boric acid contribution and equation for total absorption. *The Journal of the Acoustical Society of America*, **72** (6), 1879, **1982**.
24. ROBINSON S.P., LEPPER P.A., HAZELWOOD R.A. Good Practice Guide for Underwater Noise Measurement, No. 133, National Measurement Office, Marine Scotland, The Crown Estate, 95, **2014**.
25. PERKOVIČ M., BATISTA M., LUIN B. Analysis and graphical presentation of ship densities. Final report, ordered by IzVRS, prepared by Faculty for maritime and transport, University of Ljubljana, 29, **2019**.
26. Final report in the frame of public order "Monitoring of dolphins in the Slovenian Sea in the reporting period 2013-2018. Ordered by the Ministry for agriculture, forestry and nutrition, prepared by Morigenos - Slovenian society for marine mammals, JN001042/2018-W01, **2019**.
27. MMO Modelled Mapping of Continuous Underwater Noise Generated by Activities. A report produced for the Marine Management Organisation, MMO Project No: 1097. ISBN: 978-1-909452-87-9, **2015**.
28. MACGILLIVRAY A., MCPHERSON C., MCPHERSON G., IZETT J., GOSSELIN J., LI Z. Modeling underwater shipping noise in the Great Barrier Reef Marine Park using AIS vessel track data. *Proceedings of Inter-nose 2014*, Melbourne, Australia, **2014**.
29. TRIGG L., CHEN F., SHAPIRO G., INGRAM S., EMBLING C. An adaptive grid to improve the efficiency and accuracy of modeling underwater noise from shipping. *Geophysical Research Abstracts*, 19, EGU2017-7171, **2017**.
30. FARCAS A., POWELL C.F., BROOKES K.L., MERCHANT N.D. Validated shipping noise maps of the Northeast Atlantic. *Science of the Total Environment*, 735, 1, **2020**.